AIP | Biomicrofluidics

Covalently immobilized biomolecule gradient on hydrogel surface using a gradient generating microfluidic device for a quantitative mesenchymal stem cell study

Zongbin Liu, Lidan Xiao, Baojian Xu, Yu Zhang, Arthur FT Mak et al.

Citation: Biomicrofluidics **6**, 024111 (2012); doi: 10.1063/1.4704522
View online: http://dx.doi.org/10.1063/1.4704522
View Table of Contents: http://bmf.aip.org/resource/1/BIOMGB/v6/i2
Published by the American Institute of Physics.

Covalently immobilized biomolecule gradient on hydrogel surface using a gradient generating microfluidic device for a quantitative mesenchymal stem cell study

Zongbin Liu,[1,2] Lidan Xiao,[1] Baojian Xu,[3] Yu Zhang,[4] Arthur FT Mak,[1] Yi Li,[4] Wing-yin Man,[5] and Mo Yang[1,a)]

[1]*Interdisciplinary Division of Biomedical Engineering, Faculty of Engineering, the Hong Kong Polytechnic University, Hong Kong, People's Republic of China*
[2]*Shenzhen Institutes of Advanced Technology, Chinese Academy of Sciences, People's Republic of China*
[3]*Shanghai Institute of Microsystem and Information Technology, People's Republic of China*
[4]*Institute of Textiles and Clothing, the Hong Kong Polytechnic University, Hong Kong, People's Republic of China*
[5]*Department of Applied Biology and Chemical Technology, The Hong Kong Polytechnic University, Hong Kong, People's Republic of China*

(Received 7 February 2012; accepted 2 April 2012; published online 13 April 2012)

Precisely controlling the spatial distribution of biomolecules on biomaterial surface is important for directing cellular activities in the controlled cell microenvironment. This paper describes a polydimethylsiloxane (PDMS) gradient-generating microfluidic device to immobilize the gradient of cellular adhesive Arg-Gly-Asp (RGD) peptide on poly (ethylene glycol) (PEG) hydrogel. Hydrogels are formed by exposing the mixture of PEG diacrylate (PEGDA), acryloyl-PEG-RGD, and photo-initiator with ultraviolet light. The microfluidic chip was simulated by a fluid dynamic model for the biomolecule diffusion process and gradient generation. PEG hydrogel covalently immobilized with RGD peptide gradient was fabricated in this microfluidic device by photo-polymerization. Bone marrow derived rat mesenchymal stem cells (MSCs) were then cultured on the surface of RGD gradient PEG hydrogel. Cell adhesion of rat MSCs on PEG hydrogel with various RGD gradients were then qualitatively and quantitatively analyzed by immunostaining method. MSCs cultured on PEG hydrogel surface with RGD gradient showed a grated fashion for cell adhesion and spreading that was proportional to RGD concentration. It was also found that 0.107–0.143 mM was the critical RGD concentration range for MSCs maximum adhesion on PEG hydrogel. [http://dx.doi.org/10.1063/1.4704522]

I. INTRODUCTION

In the design of biomaterial interfaces to control cell response, efforts have focused on tuning surface chemistry. The microfluidic method has great potential to precisely modulate cell microenvironment. Traditional methods for generating microscale gradients include the glass micropipettes,[1,2] or the Boyden chamber,[3] which cannot precisely control the gradients for quantitative analysis. Recently, many efforts have been spent to use microfluidic technology to generate biomolecule gradients with advantages of reproducibility, high-throughput, and high precision.[4–7] However, current microfluidic approaches for cell study focus on culturing cells on glass or plastic substrates with gradients of diffusible proteins or surface-bound biomolecules.[8–11] In native tissues, cells always interact with the surrounding microenvironment with various biophysical properties.[12,13] So, it is preferred to use more physiological cell culture substrate to better mimic the natural cell microenvironment. Due to the high water content and

a)Author to whom correspondence should be addressed. Electronic mail: htmems@polyu.edu.hk.

tissue-like elasticity, hydrogel has been used to fabricate scaffold for cellular and tissue engineering.[14,15] The combination of protein-resistant property and grafting of bioactive ligands make it possible to control cell microenvionment for cell specific interaction study.[16–18]

Mesenchymal stem cells (MSCs) are the adult stem cells, which have the ability to differentiate into cells including osteoblasts, adipocytes, and chondrocytes.[19,20] MSCs can differentiate into different cells with ectodermal and endodermal characteristics, suggesting the possibility of MSCs for cell replacement and tissue regeneration.[21–25] The previous MSC research has focused on the effects of soluble cues, such as growth factors and cytokines.[26] However, there are increasing interests on understanding how extracellular matrix (ECM) components influence MSC behaviour and properties.[27,28] Cells respond to the external stimuli via the cell adhesion peptide such as RGD (arginine-glycine-aspartic acid) in ECM proteins and transfer the signal to the cytoskeleton to influence many cell functions including adhesion, proliferation, and differentiation.[29] The ECM protein gradient naturally presented in the cell microenvironment is a crucial signaling mechanism to direct stem cell fate.[30] Recent studies on MSC have demonstrated that RGD peptide not only enhances MSC adhesion but also modulate the intracellular mechanism for stem cell proliferation and differentiation.[31,32] It was also shown that the increase of lateral spacing of immobilized RGD peptides on the substrate would decrease MSC focal adhesion formation and spreading degree and finally decrease MSC osteogenesis on the substrate.[33] However, these studies are based on traditional culture methods with substrates of uniform concentrations, which lack peptide gradient profiles to precisely study MSC cell responses. So far, there is few report to explore RGD gradient effect on stem cell behaviour. So, it is necessary to use gradient hydrogel as a screening tool to study RGD gradient effect on MSC behaviour quantitatively.

In this paper, the poly (ethylene glycol) (PEG) hydrogel with gradient presentation of RGD peptide is fabricated to study the various concentration gradient effects on rat bone marrow derived MSCs adhesion and spreading. A quantitative analysis method is also developed to derive the critical concentration of RGD peptide for MSC adhesion based on distribution of cell adhesion density and cell spreading area on gradient hydrogel. RGD peptide can be incorporated covalently into PEG hydrogel by reaction with acryloyl-PEG-NHS to form acryloyl-PEG-RGD. The covalently immobilized RGD gradient is formed using a PDMS microfluidic gradient generator by injecting the hydrogel precursor solutions with or without acryloyl-PEG-RGD and then locked by photo-polymerization in the presence of photo-initiator. Rat bone marrow derived MSCs were then cultured on the surface of RGD gradient PEG hydrogel. Adhesion of MSCs on PEG hydrogel with various RGD gradients was then qualitatively and quantitatively analyzed by immunostaining method.

II. MATERIALS AND METHODS

A. Incorporation of RGD peptide to PEG molecule

Arg-Gly-Asp (RGD) peptide (Sigma-Aldrich, Inc., Louis, MO 63103, USA) was incorporated into PEG molecule by reacting –NHS group of acryloyl-PEG-NHS (3400 Da, Laysan Bio Inc., AL, USA) with $-NH_2$ group of the peptide as shown on Fig. 1(a). RGD and acryloyl-PEG-NHS powder were first mixed at a ratio of 3:1, and added into 10 mM sodium bicarbonate buffer solution to react for 6 h at room temperature. Excessive RGD was used to let RGD peptide react with acryloyl-PEG-NHS completely. Then, dialysis tube (Cellulose membrane with MWCO 1200, Sigma-Aldrich, Inc., Louis, MO 63178, USA) was used to dialysis the incorporated solution for one day. Finally, the dialyzed solution was dried in a vacuum freeze dryer by lyophilization for 7 h to get the acryloyl-PEG-RGD powder.

B. Fabrication of microfluidic gradient generator

The microfluidic gradient generator is based on the original design proposed by Whitesides group shown in Fig. 1(b).[34] This microfluidic gradient generator has two inlets, seven branch channels, one cell culture chamber for gradient generation and one outlet. The width of the microchannel is 100 μm. The gradient chamber connected to the outlet has a width of 2 mm

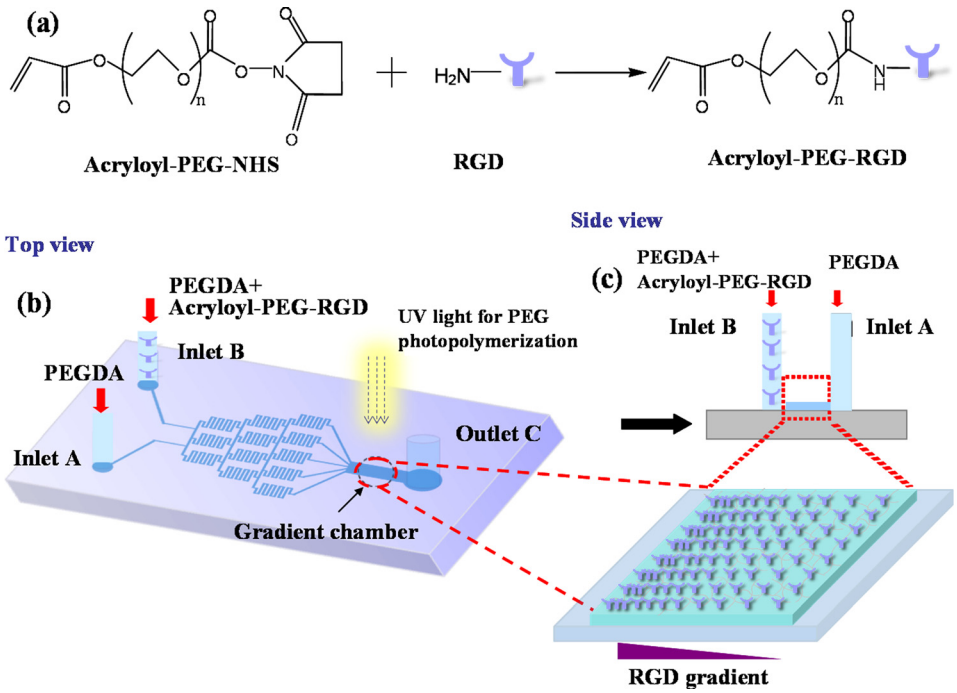

FIG. 1. (a) Conjugation of RGD with acryloyl-PEG_NHS to form acryloyl-PEG-RGD. (b) The schematic of the microfluidic gradient generator. (c) The formation of PEG hydrogel with RGD gradient using the microfluidic gradient generator.

and a length of 5 mm. The height of channel is 150 μm. Negative photoresist SU-8 (Micro-Chem Corp., Newton, MA) was used to fabricate the master on Si wafer using a photomask. The SU-8 master on Si wafer was then used to fabricate the PDMS (Sylgard 184 silicone elastomer kit, Dow Corning) microfluidic gradient generator with soft lithography method. Glass slides were surface modified with 3-(Trimethoxysilyl)propyl methacrylate (Sigma-Aldrich, Inc., USA) to make the surface reactive, which could covalently bond with the PEG hydrogel in the process of hydrogel fabrication. The PDMS and modified glass slides were finally covalently bonded by plasma treatment.

C. Simulation of gradient formation

The biomolecule gradient formation inside the microfluidic gradient generation system was analyzed using a multiphysics modeling software for computational fluid dynamics (CFD) simulation in order to estimate the generated concentration gradient profiles of PEG-RGD in the final cell culture chamber. A 2D model of the microfluidic system was established. Two modules were selected for this CFD-simulation including the flow module and chemistry/mixing module. The flow module enabled the type of motion present inside the system to be determined and the profile of velocity to be analyzed through the Navier-Stokes equations for an isothermal incompressible fluid. The second module allowed the PEG-RGD concentration gradient with diffusion coefficient to be calculated through Fick's law, using the velocity calculated from the Navier-Stokes equations as an input. To carry out the simulation, the following constants and boundary condition were imposed. The two input concentrations C_1 and C_2 were initially set to be $C_1 = 0$ and $C_2 = 1$. It is also assumed that the viscosity and density of the PEG-RGD medium are almost identical to that of water. The fluid dynamic boundary conditions imposed within CFDRC were slip at all walls and zero pressure or resistance to flow at the outlet of the device. The diffusion coefficient for PEG_{3400}-RGD (MW = 3700) was assumed to be similar to that of PEG molecule with the same molecular weight which is around 1×10^{-10} m^2/s.[35,36] The temperature was set to 300 K.

D. Characterization of gradient formation

The RGD gradient can be generated using the PDMS microfluidic gradient generator. One inlet was connected to a syringe with poly(ethylene glycol) diacrylate (PEGDA, 3400 Da, Laysan Bio Inc., AL, USA) macromer solution mixed with fluorescein isothiocyanate (FITC) labeled RGD-PEG-acryloyl. Another inlet was connected to a syringe with only PEGDA solution. The two solutions were simultaneously injected into the microfluidic generator and flowed through the microfluidc channels. At the outlet of network, the mixed solution with gradient flowed into the rectangular region (2 mm × 5 mm). When the stable RGD gradient was formed, the photo-polymerization was performed through UV irradiation (365 nm, 10 mW/cm^2) for 1 min. The gradient profile was then observed and analyzed under a fluorescence microscope. Various flow rates were tried to find the optimal flow rate to achieve the stable gradient rapidly.

E. RGD gradient PEG hydrogel generation

Fig. 1(c) shows the process for formation of RGD gradient in PEG hydrogel using the microfluidic gradient generator. Poly(ethylene glycol) diacrylate (PEGDA, 500 Da, Sigma-Aldrich, Inc., Louis, MO 63103, USA) was dissolved into phosphate buffered saline (PBS) solution at a ratio of 30:70 (V/V). Photoinitiator Irgacure 2959 was dissolved into ethanol at a concentration of 10% (W/V). The photoinitiator solution was then added into the PEGDA solution with a concentration of 0.1% (W/V). Stocked acryloyl-PEG-RGD solution (10 mM) was finally added into the PEGDA solution to prepare the solution with different RGD concentrations. Prepared PEGDA solution without acryloyl-PEG-RGD was filled in one inlet, while the other one was filled with PEGDA solution mixed with acryloyl-PEG-RGD of 0.25 mM, 0.5 mM, 1 mM, or 2 mM in the microfluidic gradient generator, respectively. Once a stable RGD gradient solution was formed in the microfluidic channel, the PEG solution in the microfluidic device was then exposed to UV light (365 nm, 200 mW/cm^2) for 1 min for photo-polymerization of RGD gradient PEG hydrogel. The hydrogel was then put into a Petri dish filled with PBS solution.

F. MSCs culture

Sprague-Dawley rat of around 7-month old was sacrificed after the intraperitoneal injection of anaesthetic drug (Ketamine and xylazine in 80 mg/kg and 8 mg/kg). Both left and right femur were removed and sterilized by 70% ethanol. The epiphyseal plate next to the femur head was removed. A syringe was used to flush the marrow with DMEM (Dulbecco's Modified Eagle Medium) supplemented with fetal bovine serum and 1% penicillin and streptomycin. The marrow solution was filtered with a cell strainer (70 μm, Falcon, USA) and then centrifuged in a 1.077 g/ml Percoll (Sigma-Aldrich, USA) density gradient at 500 g for 10 min. The enriched cells were then collected and re-suspended in tissue culture medium. The cells were then cultured in a culture flask and incubated in a humidified incubator supplemented with 5% CO_2 at 37 °C. The non-adherent cells were removed after two days culture, leaving the adherent mesenchymal stem cells in the culture flask. Cells were passaged with 0.025% trypsin-EDTA (ethylenediaminetetraacetic acid). Passage 3 cells were trypsinized, centrifuged, and used for culture on PEG hydrogel.

The PEG hydrogel in the Petri dish was first sterilized under UV light for 5 h. After sterilization, PBS solution was removed and replaced by low-glucose Dulbecco's modified Eagle medium supplemented with 10% FBS, 1% penicillin/streptomycin, 0.25% gentamicin, and 0.25% fungizone. MSCs were then seeded onto the PEG hydrogel surface with initial cell seeding density about 6×10^4 cells/cm^2. The PEG hydrogel with seeded stem cells was then incubated in a humidified incubator supplemented with 5% CO_2 at 37 °C. Cell culture medium was changed every two or three days.

G. Fluorescence staining and analysis

Actin and nucleus staining were done to characterize MSCs adhesion on PEG hydrogel surface. Phalloidin–Tetramethylrhodamine B isothiocyanate (Sigma-Aldrich, Inc., USA), which

was used to stain cell actin filament, was diluted and added to each of samples for 30 min. Diluted 4', 6-diamidino-2-phenylindole, dihydrochloride (DAPI) D1306 (Invitrogen Corporation, USA) was then added to each sample for 5 min. DAPI was used for staining the cell nuclei. Fluorescence images of stained cells were then recorded by a Nikon Eclipse 80i fluorescence microscope (Nikon, Japan). Cell spreading degree is quantified by measuring the cell adhesion area from the actin staining images. All the imaging processing to determine the cell adhesion area is based on the imaging toolbox of MATLAB (MathWorks, USA). The nucleus stained fluorescence image is first used to determine each cell position and count the total cell number. Then, based on the position of each single cell, the actin stained fluorescence image is used to outline the perimeter of each single cell and calculate the cell adhesion area. The image of overlapping cells could be split into single ones using imaging processing toolbox of MATLAB based on the combination of edge detection process and pseudo-color technique with color space extraction.

III. RESULTS

A. Simulation

Using the CFD simulation software, the diffusion inside the microfluidic device was analyzed in details. To generate the stable concentration gradient in the cell culture chamber in the downstream of the mixing channels, it is required that the flow inside the microchannels is fully developed and the stable gradient can be formed within a few minutes. Fig. 2(a) shows that the complete mixing inside the microfluidic channels for the flowing speed of 8 μl/min is achieved within three cycles of curing microchannels. In this case, the flowing speed of 8 μl/min can achieve the low Reynolds number around 1 for laminar flow. Fig. 2(b) shows the time evolution

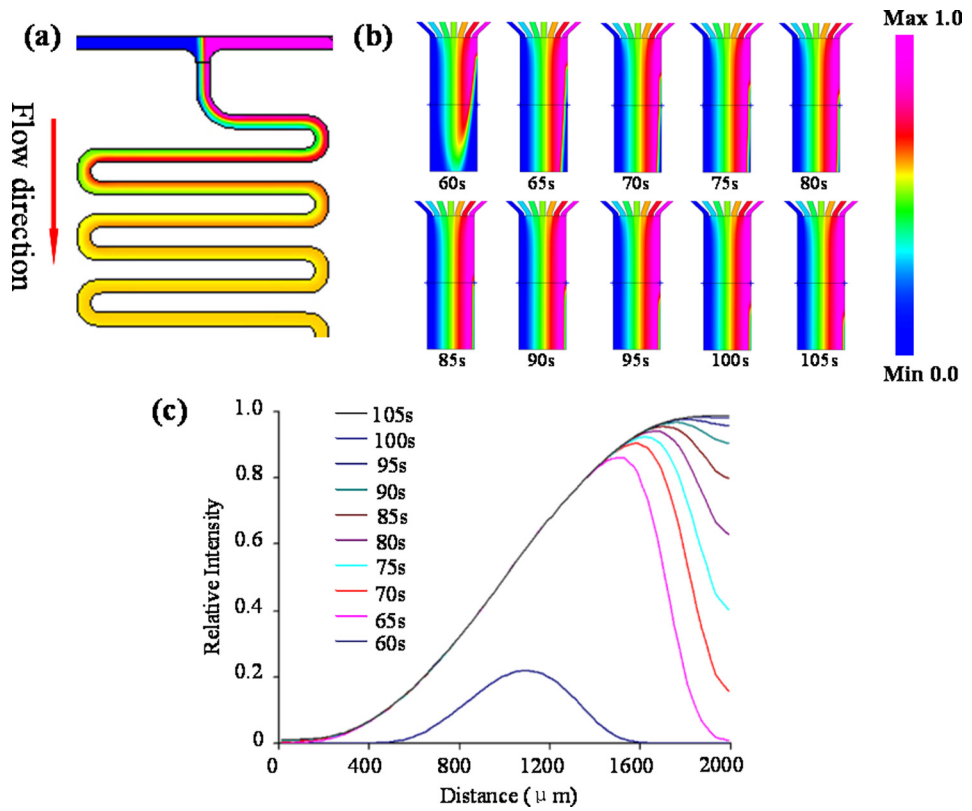

FIG. 2. (a) Simulation of mixing within the microchannels. Arrow shows the flow direction. (b) Time evolution of the concentration gradient in the cell culture chamber with the flowing speed of 8 μl/min. (c) Time evolution of concentration profiles for the mid-plane in the cell culture chamber. It takes around 2 min for the concentration gradient to reach stability.

of the concentration gradient in the cell culture chamber with the flowing speed of 8 μl/min. Fig. 2(c) shows the detailed gradient profiles. It demonstrated that the stable concentration gradient could be achieved around 2 min in the whole cell culture chamber after the injection of solution into the microfluidic gradient generator.

B. Gradient characterization

Fig. 3(a) shows the fabricated microfluidic gradient generator. Various RGD concentration gradient hydrogels were generated including 0–0.25 mM gradient hydrogel with a gradient of 0.125 mM/mm, 0–0.5 mM gradient hydrogel with a gradient of 0.25 mM/mm, and 0–1 mM gradient hydrogel with a gradient of 0.5 mM/mm. To visualize the gradient, fluorescence labelled RGD-PEG-acryloyl was synthesized using FITC as the fluorescent probe. The microchannels were first filled with ethanol until no air bubbles were observed. And then DI water was used to wash the microchannels several times. At time t = 0, 0.5 mM FITC labelled RGD-PEG-acryloyl mixed PEGDA solution and pure PEGDA solution was injected into the microfluidic channels through the two inlets by a syringe pump. It took around 2 min for the gradient to reach steady state when the flow speed is set to be 8 μl/min. Fig. 3(b) shows the fluorescence intensity gradient formed in the cell culture chamber at t = 120 s for 0–0.25 mM gradient hydrogel. A linear gradient profile in the middle of the cell culture chamber is shown in Fig. 3(c), which matches well with the simulated gradient curve. The RGD gradient was then fixed by exposure to UV light (365 nm, 200 mW/cm^2) for 1 min.

C. Stem cell culture on RGD gradient PEG hydrogel

MSCs were then cultured on RGD gradient PEG hydrogel with an initial cell density of 6×10^4 cells/cm^2 in an incubator. We first explored how the various RGD concentrations on a fixed gradient slope curve of 0.125 mM/mm (0–0.25 mM over 2000 μm) affect cell morphology, cell adhesion density, and cell covering area distribution across the hydrogel. Actin and nuclear staining were performed to show the effect of RGD gradient on cell adhesion. The nuclear staining images show the distribution of cell number and actin staining images show the cell morphology and spreading degree on RGD gradient PEG hydrogel surface. Fig. 4 shows stem cell adhesion on PEG hydrogel with a RGD gradient of 0.125 mM/mm (0–0.25 mM over

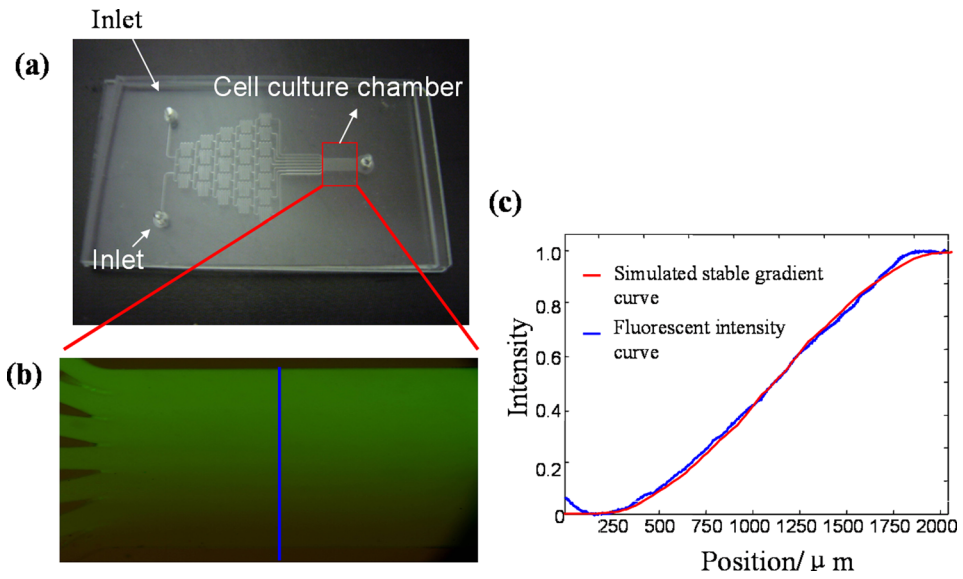

FIG. 3. (a) The fabricated PDMS microfluidic gradient generator. (b) Fluorescence image of FITC labeled RGD stable gradient formed in the cell culture chamber. (c) The linear fluorescence intensity gradient formed at the mid-plane of the cell culture chamber and the related simulated gradient curves at t = 120 s.

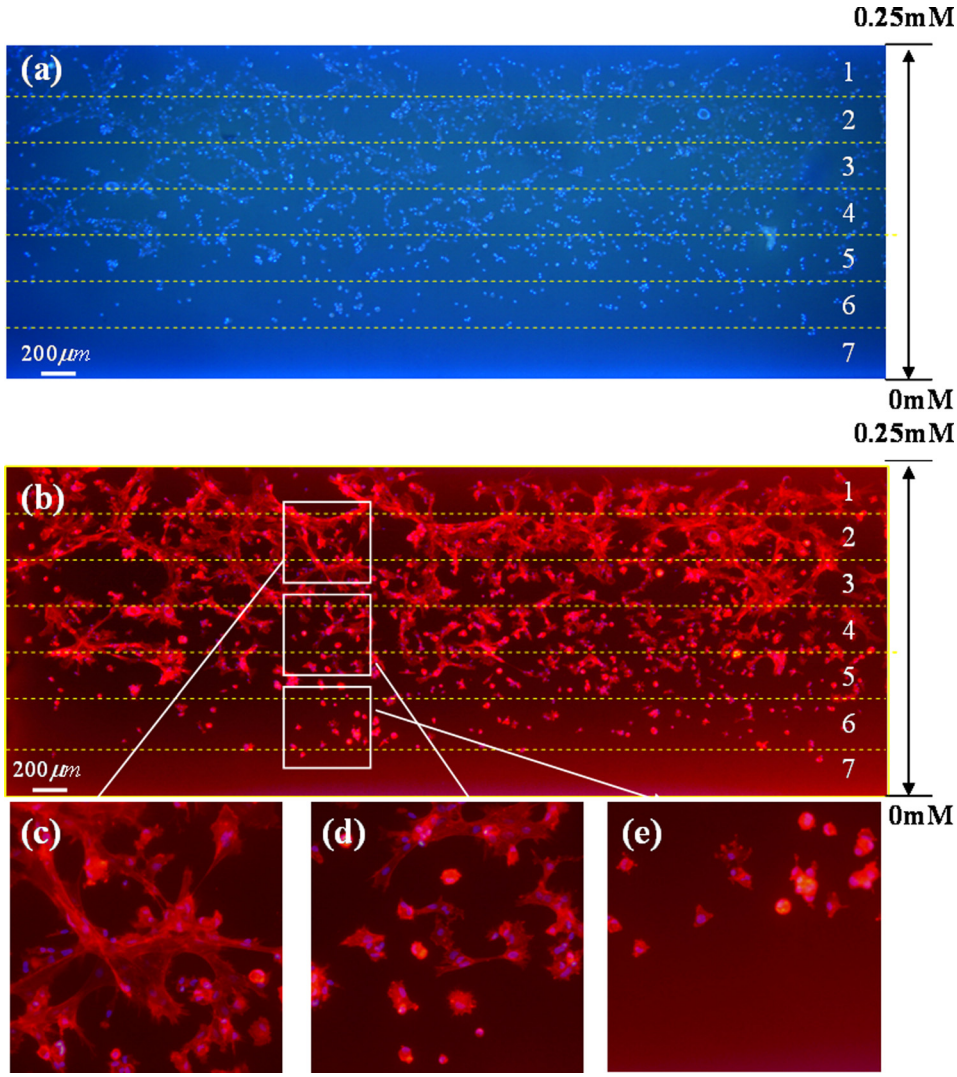

FIG. 4. (a) The nuclear staining image shows a gradient distribution of cell number on PEG hydrogel with 0–0.25 mM gradient of RGD (b) The actin staining image shows a gradient distribution of cell spreading on PEG hydrogel with 0–0.25 mM gradient of RGD. (c) At the high RGD concentration, MSCs showed good spreading morphology. (d) At the intermediate RGD concentration region, the spreading degree of cells decreased. (e) At the low RGD concentration region, MSCs showed rounding shape.

2000 μm) after 1 day culture by washing away the unattached cells. The hydrogel samples were gently washed with PBS solution for several times before taking the fluorescence images. Since it was hard to thoughtfully wash the bonding side between PEG hydrogel and glass slide, the fluorescence background of hydrogel is a little strong. The nuclear staining image shows a gradient distribution of cell number on RGD gradient PEG hydrogel (Fig. 4(a)). On the low RGD concentration area (bottom area of the PEG hydrogel), there were few cells adhered on the surface. With the increase of RGD concentration, more cells could adhere on the surface. Moreover, adherent cells show s gradient distribution for the spreading on the hydrogel surface along the RGD concentration gradient (Fig. 4(b)). On the top area of hydrogel with the highest RGD concentration, the stem cell fully spread with a protruding lamellopodia edge (Fig. 4(c)). The spreading degree of cells decreased in the intermediate concentration region (Fig. 4(d)). In the lowest RGD concentration region, cells did not spread well with a rounded up morphology (Fig. 4(e)). For the quantitative analysis of cell adhesion including cell density and cell covering area, we subdivided the whole gradient region into 7 equal blocks (Figs. 4(a) and 4(b)).

The nucleus staining image of cells on RGD gradient PEG hydrogel could be used to calculate the cell adhesion density.

The number of MSCs on each block was counted and the average cell density was calculated. Fig. 5(a) shows the cell adhesion density on 0–0.25 mM RGD gradient PEG hydrogel. It can be seen that the adherent cell number on block 7 was nearly zero, which is the lowest RGD concentration. With the increase RGD concentration from block 6 to block 2, the cell density increased accordingly, which showed a correlation between the adherent MSCs density and RGD concentration. There was a slight decrease of cell density in block 1 compared with block 2. This may be due to the boundary effect of non-flat hydrogel surface of block 1, which can make it difficult for cells to adhere on the surface. Another interesting phenomenon was that there was no big difference for cell adhesion density from blocks 1 to 4. This may be caused by the saturation of cell adhesion.

Fig. 5(b) shows the average single cell adhesion area distribution on 0–0.25 mM RGD gradient PEG hydrogel. The cell adhesion area indicates the cells spreading degree. If cells have better spread morphology, they will have more adhesion covering area. The average single cell adhesion area was calculated from actin staining images of MSCs on PEG hydrogel. The single cell adhesion area was divided into 3 categories: 0–500 μm^2, 500–1000 μm^2, and $\geq$1000 μm^2. The diameter of MSC in this experiment is around 20 μm and the rounded MSC surface area is

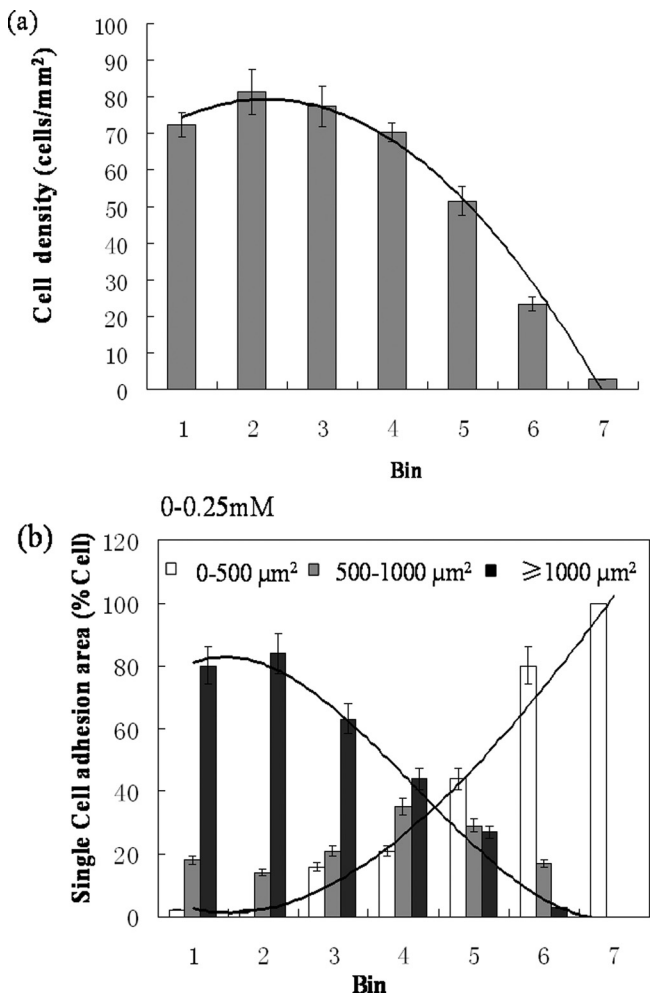

FIG. 5. Quantitative analysis of MSCs adhesion on PEG hydrogel with 0–0.25 mM RGD gradient. (a) Adherent cell density distribution based on nuclear staining image and (b) single cell adhesion area distribution based on actin staining image.

around 300–400 μm^2. So, the adhesion area of most unspread cells should be under 500 μm^2. For this reason, 0–500 μm^2 is used as "least spread" category, 500–1000 μm^2 is used as "medium spread" category, and >1000 μm^2 is treated as "most spread" category. In each block, the ratio of cell adhesion area for each category was calculated. From the diagram in Fig. 5(b), it could be seen that the average single cell adhesion area on blocks 1–3 were mostly larger than 1000 μm^2, which demonstrated good spreading on hydrogel surface. Block 4 was the transition region, where around 44% of single cell adhesion area was larger than 1000 μm^2, 35% was between 500–1000 μm^2 and 21% was under 500 μm^2. On blocks 5–7, the single cell adhesion area was mostly less than 500 μm^2. The above analysis indicated that the single cell adhesion area decreased with the decrease of RGD concentration in the gradient hydrogel. The trendlines for single cell area under 500 μm^2 and larger than 1000 μm^2 were also shown in Fig. 5(b). The crosspoint of the two trendlines could be used as an indicator for the critical concentration, where is around block 4. From both cell density and cell spreading degree analysis, it is concluded that block 4 with the RGD concentration around 0.107–0.143 mM is the critical concentration range for MSCs to reach excellent adhesion.

D. Stem cell adhesion on PEG hydrogel with various RGD gradients

We then explored how the gradient slope change affected MSC cell adhesion density and cell covering area distribution across the hydrogel using various RGD gradient slopes of 0.125 mM/mm (0–0.25 mM/2000 μm), 0.25 mM/mm (0–0.5 mM/2000 μm), and 0.5 mM/mm (0–1 mM/2000 μm). Fig. 6 shows MSCs adhesion on PEG hydrogel with RGD gradients of 0-0 mM, 0–0.25 mM, 0–0.5 mM, and 0–1 mM after 1 day culture by washing away the unattached cells. For PEG hydrogel with 0-0 mM RGD gradient, there were few cells attached (Fig. 6(a)) and actin filament was barely observed on the surface (Fig. 6(b)). A sharp gradient distribution of both cell number and cell spreading degree was observed for PEG hydrogel with 0–0.25 mM

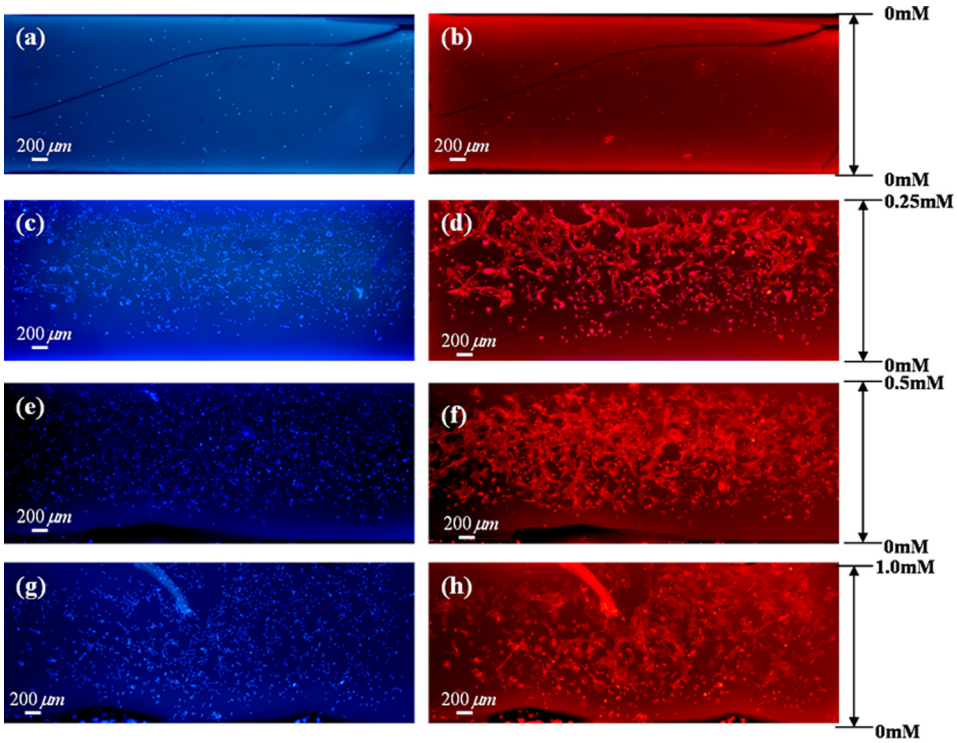

FIG. 6. Nuclei and actin staining images of MSCs on various RGD gradients. (a) Nuclei staining image of 0-0 mM; (b) Actin staining image of 0-0 mM; (c) Nuclei staining image of 0–0.25 mM; (d) Actin staining image of 0–0.25 mM; (e) Nuclei staining image of 0–0.5 mM; (f) Actin staining image of 0–0.5 mM; (g) Nuclei staining image of 0–1 mM; (h) Actin staining image of 0–1 mM.

gradient (Fig. 6(c) and 6(d)). With the increase of RGD gradient to 0–0.5 mM, more cell adhesion saturation areas were observed and the gradient distribution for cell adhesion was not so obvious (Figs. 6(e) and 6(f)). When the RGD gradient increased to 0–1 mM, there was no observable gradient distribution for cell adhesion in the whole PEG hydrogel region (Figs. 6(g) and 6(h)).

Using the similar quantitative analysis method, the cell density distribution on the PEG hydrogel with RGD gradients of 0–0.25 mM, 0–0.5 mM, and 0–1 mM is shown in Fig. 7(a). The fitting trendlines are also shown in Fig. 7(a). It is shown that the critical saturation concentration for the whole range of 0–0.5 mM gradient hydrogel is on block 6 in the range of 0.07–0.143 mM, and the critical saturation concentration for the whole range of 0–1.0 mM

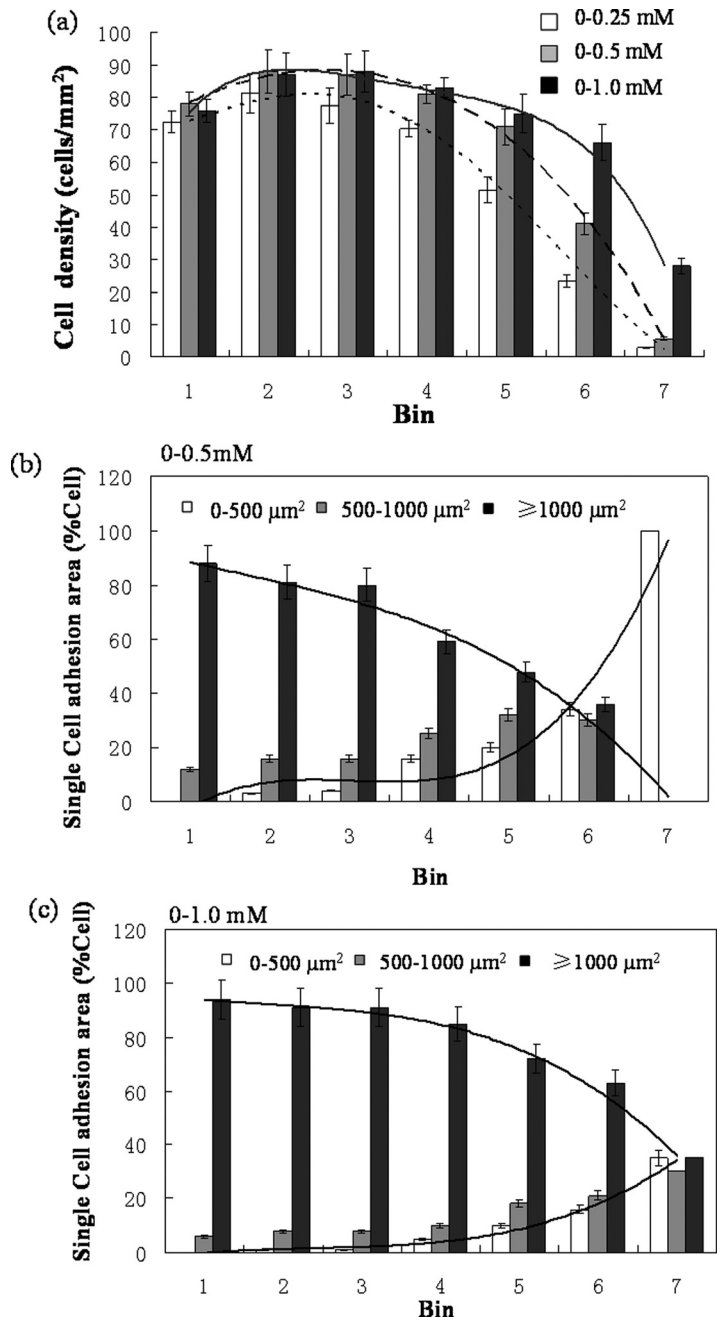

FIG. 7. (a) Adherent cell density distribution on various RGD gradient of 0–0.25 mM, 0–0.5 mM, and 0–1 mM. (b) Single cell adhesion area distribution on 0–0.5 mM. (c) Single cell adhesion area distribution on 0–1.0 mM.

gradient hydrogel is on block 7 in the range of 0–0.143 mM. Figs. 7(b) and 7(c) show the average single cell adhesion area distribution on PEG hydrogel with 0–0.5 mM and 0–1 mM RGD gradients. The crosspoints of the trendlines for single cell area under 500 μm^2 and larger than 1000 μm^2 also confirmed that the critical concentrations were on block 6 for 0–0.5 mM gradient and on block 7 for 0–1 mM gradient, respectively. These critical concentration ranges for MSCs adhesion match that derived from 0 to 0.25 mM gradient, which is around 0.107–0.143 mM. Obviously, 0–0.25 mM gradient has the largest linear response region which could be used to narrow down the range to precisely determine the critical concentration for MSCs excellent adhesion.

IV. CONCLUSIONS

In this study, a PDMS microfluidic gradient generator was designed to generate a stable and controllable concentration gradient in the PEG pre-polymer solution in a short time. We then fabricate PEG hydogel with various linear gradient concentration profiles of immobilized RGD peptide using photopolymerization method. The RGD gradient effects on rat MSCs adhesion were explored by culturing MSCs on PEG hydrogel surfaces with various RGD gradient profiles. Quantitative analysis was performed for both cell density and cell spreading area distribution along RGD gradient. The RGD critical concentration for MSCs excellent adhesion can be precisely determined using this quantitative analysis method by choosing the appropriate gradient profile. The recent research has shown that the cell adhesion peptide such as RGD peptide not only enhances stem cell adhesion but also guide stem cell other functions such as proliferation and differentiation by transferring the external signals to the cytoskeleton.[30] It is also demonstrated that RGD peptide could enhance MSC stem cells osteogenesis.[31,32] The spatial distribution of RGD peptide immobilized on the substrate could affect MSC focal adhesion formation and spreading degree, which in turn correlate with MSC osteogenesis. So, this microfluidic peptide gradient hydrogel platform together with the quantitative analysis method provides potential platforms not only for the stem cell adhesion but also for the study of peptide gradient effects on stem cell differentiation.

ACKNOWLEDGMENTS

This work was partially supported by the postdoctoral fellowship fund of the Hong Kong Polytechnic University (G-YX5G).

[1]J. Q. Zheng, M. Felder, J. A. Connor, and M. M. Poo, Nature (London) **368**, 140 (1994).
[2]A. M. Lohof, M. Quillan, Y. Dan, and M. M. Poo, J. Neurosci. **12**, 1253 (1992).
[3]S. Boyden, J. Exp. Med. **115**, 453 (1962).
[4]B. G. Chung, F. Lin, and N. L. Jeon, Lab Chip **6**, 764 (2006).
[5]S. K. W. Dertinger, D. T. Chiu, N. L. Jeon, and G. M. Whitesides, Anal. Chem., **73**, 1240 (2001).
[6]Y. Huang, B. Agrawal, D. D. Sun, J. S. Kuo, and J. C. Williams, Biomicrofluidics **5**, 013412 (2011).
[7]N. L. Jeon, H. Baskaran, S. K. W. Dertinger, G. M. Whitesides, L. Van de Water, and M. Toner, Nat. Biotechnol. **20**, 826 (2002).
[8]E. Delamarche, A. Bernard, H. Schmid, A. Bietsch, B. Michel, and H. Biebuyck, J. Am. Chem. Soc. **120**, 500 (1998).
[9]K. A. Fosser and R. G. Nuzzo, Anal. Chem. **75**, 5775 (2003).
[10]W. Georgescu, J. Jourquin, L. Estrada, A. R. A. Anderson, V. Quaranta, and J. P. Wikswo, Lab Chip **8**, 238 (2008).
[11]R. C. Gunawan, E. R. Choban, J. E. Conour, J. Silvestre, L. B. Schook, H. R. Gaskins, D. E. Leckband, and P. J. A. Kenis, Langmuir **21**, 3061 (2005).
[12]A. J. Gaarcia, Biomaterials **26**, 7525 (2005).
[13]D. E. Discher, P. Janmey, and Y. L. Wang, Science **310**, 1139 (2005).
[14]K. T. Nguyen and J. L. West, Biomaterials **23**, 4307 (2002).
[15]N. A. Peppas, Y. Huang, M. Torres-Lugo, J. H. Ward, and J. Zhang, Annu. Rev. Biomed. Eng. **2**, 9 (2000).
[16]C. R. Nuttelman, M. C. Tripodi, and K. S. Anseth, J. Biomed. Mater. Res. Part A. **68**, 773 (2004).
[17]X. Z. Shu, K. Ghosh, Y. Liu, F. S. Palumbo, Y. Luo, R. A. Clark, and G. D. Prestwich, J. Biomed. Mater. Res. Part A. **68**, 365 (2004).
[18]J. K. Tessmar and A. M. Gopferich, Macromol. Biosci. **7**, 23 (2007).
[19]A. I. Calplan Tissue Eng. **11**, 1198 (2005).
[20]L. Jackson, D. R. Jones, P. Scotting, and V. Sottile, J. Postgrad. Med. **53**, 121 (2007).
[21]S. P. Bruder, A. A. Kurth, M. Shea, W. C. Hayes, N. Jaiswal, and S. Kadiyal, J. Orthop. Res. **16**, 155 (1998).
[22]M. Krampera, G. Pizzolo, G. Aprili, and M. Franchini, Bone **39**, 678 (2006).
[23]D. S. Benoit, M. P. Schwartz, A. R. Durney, and K. S. Anseth, Nature Mater. **7**, 816 (2008).

[24]F. Yang, C. G. Williams, D. A. Wang, H. Lee, P. N. Manson, and J. Elisseeeff, Biomaterials **26**, 5991 (2005).
[25]D. S. Benoit, A. R. Durney, and K.S. Anseth, Biomaterials **28**, 66 (2007).
[26]J. M. Curran, R. Chen, and J. A. Hunt, Biomaterials **27**, 4783 (2006).
[27]A. A. Sawyer, K. M. Hennessy, and S. L. Bellis, Biomaterials **26**, 1467 (2005).
[28]E. A. Cavalcanti-Adam, I. M. Shapiro, R. J. Composto, E. J. Macarak, and C. S. Adams, J. Bone Miner. Res. **17**, 2130 (2002).
[29]B. Geiger and A. Bershadsky, Cell **110**, 139 (2002).
[30]M. P. Lutolf, P. M. Gilbert, and H. M. Blau, Nature (London) **462**, 433 (2009).
[31]H. Shin, K. Zygourakis, M. C Farach-Carson, M. J Yaszemski, and A. G. Mikos, J. Biomed. Mater. Res. **69**, 535 (2004).
[32]H. Shin, J. S. Temenoff, G. C. Bowden, K. Zygourakis, M. C. Farach-Carson, M. J. Yaszemski, and A. G. Mikos, Biomaterials **26**, 3645 (2005).
[33]J. E. Frith, R. J. Mills, and J. J. Cooper-White, J. Cell Sci. **125**, 1 (2012).
[34]N. L. Jeon, S. K. W. Dertinger, D. T. Chiu, I. S. Choi, A. D. Stroock, and G. M. Whitesides, Langmuir **16**, 8311 (2000).
[35]V. Murugaiah and R. E. Synovec, Anal. Chem. **64**, 2130 (1992).
[36]R. A. Waggoner, F. D. Blum, and J. C. Lang, Macromolecules **28**, 2568 (1995).